# Structural and phononic characteristics of nitrogenated holey graphene

H. Sahin*

*Department of Physics, University of Antwerp, Campus Groenenborgerlaan, 2020, Antwerp, Belgium*

(Received 22 June 2015; published 19 August 2015)

Recent experimental studies showed that formation of a two-dimensional crystal structure of nitrogenated holey graphene (NHG) is possible. Similar to graphene, NHGs have an atomically thin and strong crystal structure. Using first-principles calculations, we investigate the structural, phononic, and thermal properties of monolayer NHG crystal. Our charge analysis reveals that the charged holey sites of NHG provide a reactive ground for further functionalization by adatoms or molecules. We also found that similar to graphene, the NHG structure has quite high-frequency phonon modes and the presence of nitrogen atoms leads to the emergence of additional vibrational modes. Our phonon analysis reveals the presence of three characteristic Raman-active modes of NHG. Furthermore, the analysis of constant-volume heat capacity showed that the NHG structure has a linear temperature dependence in the low-temperature region. The strong lattice structure and unique thermal properties of the NHG crystal structure are desirable in nanoscale device applications.

DOI: 10.1103/PhysRevB.92.085421 PACS number(s): 81.05.ue, 73.22.Pr, 63.22.Rc, 61.48.Gh

## I. INTRODUCTION

Research on two-dimensional (2D) structural variants of graphene [1] is of prime importance due to the lack of an energy band gap, which limits its use in optoelectronic device applications. Although several 2D carbon allotropes, such as graphyne, graphdiyne, and graphenylene have been proposed by theoretical studies, experimental realization is the main drawback of these structures [2]. However, functionalization of preexisting graphene sheets is a more practical way of tuning the electronic properties of graphene rather than synthesis of new allotropes. It was demonstrated by Lahiri *et al.* that an array of lattice defects in graphene acts as a quasi-one-dimensional metallic wire [3]. In addition, Bai *et al.* showed that formation of graphene nanomeshes with a periodic array of holes can open up a band gap in graphene's electronic band dispersion [4]. It was also demonstrated that these graphene variants do not only support currents greater than individual graphene nanoribbon devices, but also have high on-off ratios. Moreover, our investigations revealed that depending on the hole-hole interactions and the atomic structure of the holes, the nanomesh can be in metallic, semiconducting or semimetallic states [5].

Another large subgroup of two-dimensional crystals is two-dimensional polymers. In these layered structures, which are mainly composed of H, C, O, and N atoms, graphenelike building blocks are linked to each other by strong covalent bonds and linker atom groups. So far rational synthesis of organic 2D materials has been achieved using several techniques, such as formation of covalent organic frameworks (COFs), surface-mediated polymerization of polyfunctional monomers, and solid-state topochemical polymerizations [6,7]. In addition, Cote *et al.* showed that COFs can be synthesized by condensation reactions of phenyl diboronic acid and hexahydroxytriphenylene. In these porous graphitic layers that are either staggered (COF-1, $P6_3/mmc$) or eclipsed (COF-5, $P6/mmm$), crystal structures are entirely held by strong bonds between B, C, and O atoms and pore sizes ranging from 7 to 27 Å [8]. In addition, Kandambeth *et al.* demonstrated that hydrogen-binding interactions play an important role in crystallinity, porosity, and chemical stability of 2D COFs [9].

Nitrogenated holey graphene (NHG) structures are the most recently synthesized two-dimensional graphene variants [10]. While the wet-chemistry-based bottom-up approach which was used for the synthesis of NHGs provides an easy and effective method, the simple atomic structure and semiconducting electronic behavior of NHGs are quite desirable features for nanodevice applications. Since NHGs are appealing materials in the area of single-layer crystal structures, identification of their characteristics is of importance for future studies in the field. Apart from the recent study of Mahmood *et al.* [10], reporting the first synthesis and electronic structure, there is no literature on NHGs. In our study we present a detailed analysis of the vibrational and thermodynamical properties of NHGs.

After the Introduction the rest of the paper is organized as follows: Computational methodology is given in Sec. II. Atomic structure and bonding characteristics of NHGs are investigated in Sec. III. Phonon dispersion, vibrational analysis, and thermal properties of single-layer NHGs are presented in Secs. IV and V, respectively. Section VI is devoted to a brief discussion of our results.

## II. COMPUTATIONAL METHODOLOGY

For geometry optimizations and determination of electronic structure of NHGs, we performed first-principles calculations within density functional theory (DFT) using the plane-wave projector-augmented wave (PAW) method [11] implemented in the Vienna *Ab-Initio* Simulation Package (VASP) [12–14]. The Perdew-Burke-Ernzerhof (PBE) [15] form of the generalized gradient approximation (GGA) was adopted to describe electron exchange and correlation. The kinetic energy cutoff for plane-wave expansion was set to 500 eV, where the hexagonal Brillouin zone (BZ) was sampled with a Γ-centered $21\times21\times1$ $k$-point grid. To avoid the interaction between adjacent NHG sheets, we put a large vacuum spacing of 15 Å in the perpendicular direction. The convergence threshold for energy was chosen as $10^{-5}$ eV and $10^{-4}$ eV/Å for energy

*hasan.sahin@uantwerpen.be

 

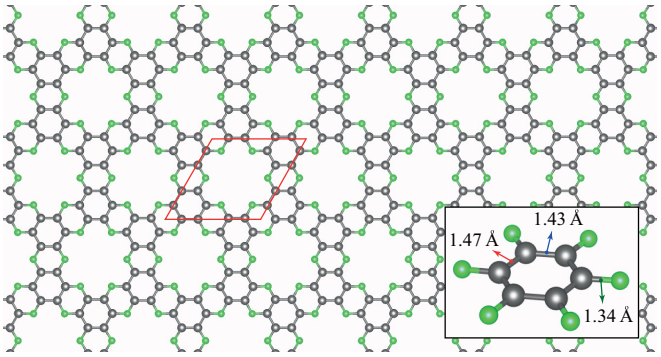


FIG. 1. (Color online) Top view of atomic structure of single-layer holey graphene. Nitrogen and carbon atoms are shown by green and gray balls, respectively. The primitive unit cell of the crystal is delineated by a red rhombus. A tilted perspective view of a N-surrounded benzene unit and bond lengths are given in the inset.

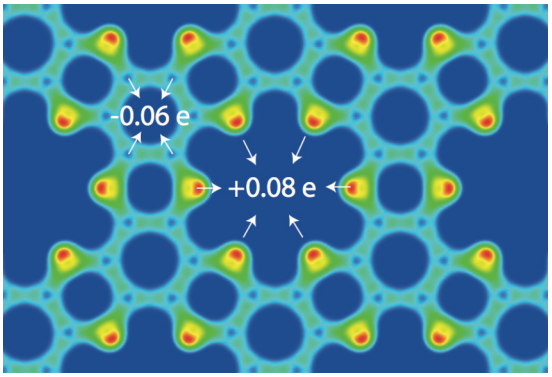


FIG. 2. (Color online) Top view of total charge density profile of NHG. Increasing charge density is shown by color scheme from blue to red. The amount of extra (missing) electron charge on N (C) atoms are shown by + (−) sign.

and force, respectively. The charge distribution on atoms was calculated by using the Bader analysis [16,17].

The vibrational spectrum of NHG is investigated via *ab-initio* phonon calculations. These are performed in the harmonic approximation by making use of the small displacement method implemented in the PHON code [18]. The phonon dispersions and thermodynamic quantities of the 72-atom supercell structure of NHG are calculated with a force field induced by a 0.01-Å displacement.

## III. STRUCTURAL PROPERTIES

The optimized structure and lattice parameters of an NHG crystal are shown in Fig. 1. In the NHG structure, just like graphene, carbon and nitrogen atoms are bonded together upon $sp^2$ hybridization. The crystal is composed of evenly distributed holes and nitrogen atoms in an atomically flat structure. Each hexagonal primitive unit cell of NHG includes 6 N and 12 C atoms and therefore it has the stoichiometry of $C_2N$. As shown in the inset of Fig. 1, the NHG structure contains one C-N bond (1.34 Å) and two kinds of inequivalent C-C bonds: the long one facing the holey side (1.47 Å) and short one located inside (1.43 Å). Here short C-C and C-N bond lengths show that the CHN crystal structure is formed through strong carbon-nitrogen hybridization and the benzene rings still have graphitic character. It is worth noting that the experimentally observed semiconducting behavior with a large (1.96-eV) band gap is a consequence of the strong carbon-nitrogen hybridization.

Calculation of the charge density profile of the optimized structure allows us to discuss how the atomic structure is formed and to deduce some of its electronic properties. In Fig. 2 we show the total charge density of whole NHG crystal structure. It is seen that the holey site of graphene is surrounded by negatively charged N atoms, while each C atom in benzene rings donates 0.06 $e$. Here each N atom is $-0.08$ $e$ charged. It is seen that the nitrogen atoms having relatively larger electronic local density of states are seen as bright spots in the scanning tunneling microscopy (STM) data measured by Mahmood *et al*. [10]. Although the NHG structure has a trigonally symmetric lattice structure that results in Dirac cones at the $K$ symmetry point, involving a second atom type opens the band gap [5]. Moreover, the holey site of NHG, which forms a hexagon with radius of 5.52 Å, provides a reactive region inside and therefore it provides a reactive ground for further functionalization by adatoms or molecules.

## IV. PHONON DISPERSION

Determination of the phonon properties of a given material not only allows us to examine its dynamical stability but also to find out the characteristic fingerprints of the structure. As we reported recently, structural reconstructions, effect of strain, Raman scattering, and thickness-dependent properties of a material can be monitored via calculation of its phonon dispersion [19,20].

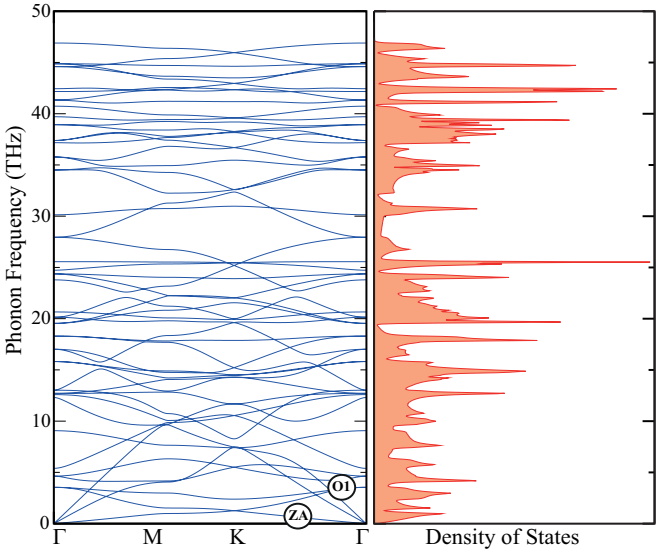


FIG. 3. (Color online) Phonon dispersion and phonon density of states of NHG crystal structure.

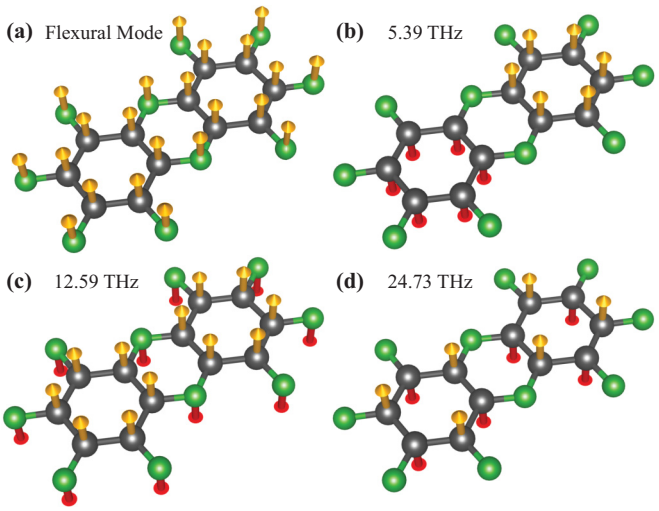


FIG. 4. (Color online) Presentation of (a) flexural acoustic (ZA) mode and (b)–(e) three Raman-active phonon modes of NHG structure. Atomic displacement directions are shown by up (yellow) and down (red) arrows.

In Fig. 3 we show both the dispersion of phonon branches of NHG and the corresponding phonon density of states. The primitive unit cell of NHG consisting of 18 atoms possesses 54 zone center phonon branches. At first sight a feature of the phonon dispersion of NHG is the linearly crossing phonon branches at the K symmetry point. It is known that such a linear crossing directly stems from the hexagonal (or trigonal) crystal symmetry [5,21–23]. As clear from Fig. 1, the NHG crystal structure possess trigonal symmetry.

At the Γ point, the first three lowest energy phonon modes are acoustic modes. Among these acoustic phonon branches the lowest energy mode is a flexural mode (labeled ZA in Fig. 3), which is a characteristic vibration mode in low-dimensional crystal structures. As presented in Fig. 4(a), the flexural mode corresponds to the periodic out-of-plane transverse motion (or bending) of the NHG surface. As it is well known from other 2D crystals such as graphene, hex-BN, silicene, and $MoS_2$, the defining characteristic of the ZA mode is its parabolic dispersion curve near the Γ point. In addition, due to the lack of neighboring atoms in the perpendicular direction, the ZA mode is the lowest-energy acoustic mode. Therefore, ZA is the easiest phonon mode to be excited and carries most of the vibrational energy. Here it is also worth mentioning that due to presence of holey sites and N linkers between the benzene rings, dispersion of the ZA mode slightly deviates from the quadratic behavior. Another important point in NHG's phonon spectrum is that similar to graphene (and differing from silicene and monolayer $MoS_2$), the ZA flexural mode couples to the lowest optical mode (labeled O1) at the K symmetry point.

The presence of optical phonon branches that have quite high eigenvalues is another direct indication of the structural stability of the NHG structure. Compared to graphene, which has the highest phonon mode at 47.97 THz (1600 $cm^{-1}$), NHG has an optical mode with eigenfrequency of 46.98 THz, which is quite high. Therefore, we can conclude that the presence of N linkers between the benzene rings forms a quite stable lattice structure through strongly hybridized N and C orbital states. It appears that the bottom-up wet-chemical reaction is not only a simple and highly efficient method for synthesis but also results in the formation of a quite strong 2D NHG network structure.

In Fig. 4, some of the characteristic NHG lattice vibrations are also presented. It is seen that the phonon mode at 5.39 THz corresponds to out-of-plane counterphase motion of neighboring benzene rings of NHG crystal. However, nitrogen atoms stay fixed in this mode. In addition, in the phonon mode at 12.59 THz nitrogen and carbon atoms have out-of-plane motion. In this mode, that has optical character, each atom type moves in opposite direction to each other. Moreover, another characteristic phonon mode is seen at 24.73 THz. In this mode, while nitrogen atoms stay fixed, each carbon atom has an out-of-plane counterphase motion with respect to the neighboring carbon atoms. Due to the their high energy and bond-stretching character, these three phonon modes are likely to be observed in Raman measurements.

## V. THERMAL PROPERTIES

Most of the unique properties of graphene and graphenelike materials, such as fluorographene and $MoS_2$, stem from their highly anisotropic nature and strong planar structure. For NHGs, one can expect that in addition to their two-dimensional structure, the presence of large vacancy and nitrogen-doped sites may lead to additional novel features.

Using phonon dispersions, as obtained in the harmonic approximation, we can also predict thermal properties of nitrogenated holey graphene structures through the calculation of heat capacity, which is one of the easy measurable quantities of a crystal structure. Moreover, it is known that the specific heat of ultrathin materials is mainly determined by the lattice vibrations (phonons) and the contribution of free conduction electrons is negligible. In Fig. 5 we present the heat capacity (at constant volume) of five different atomically thin monolayer crystal structures.

Our calculations reveal that, similar to bulk materials, NHGs and other graphenelike monolayer materials have the classical behavior, which is in agreement with Dulong-Petit law. At high temperatures, all atomic degrees of motion are excited and the specific heat of the structures are expected to approach the limit value of $3Nk_B$, where $N$ is the number of atoms per unit cell. Figure 5 shows that the specific heat of NHG and other graphene derivatives is always larger (smaller) than the single-layer $MoS_2$ at high (low) temperatures. It is seen that the larger the molar mass, the smaller the specific heat at high temperatures. In addition, Fig. 5 also reveals that the NHG crystal structure approaches the Dulong-Petit limit after fluorographene, chlorographene, and $MoS_2$ and therefore it has a larger Debye temperature.

Interestingly, the thermal properties of NHGs are quite different at low temperatures. As shown in the inset of Fig. 5, the specific heat of graphane, fluorographene, chlorographene, and $MoS_2$ rises as $T^n$ ($n > 0$). However, the specific heat of nitrogenated holey graphene has an entirely different linear dependence on the temperature. As previously reported [24], the specific heat of 2D monolayer crystals scales with $T^{2/n}$, where the phonon dispersion is $\omega = q^n$. Therefore, we can

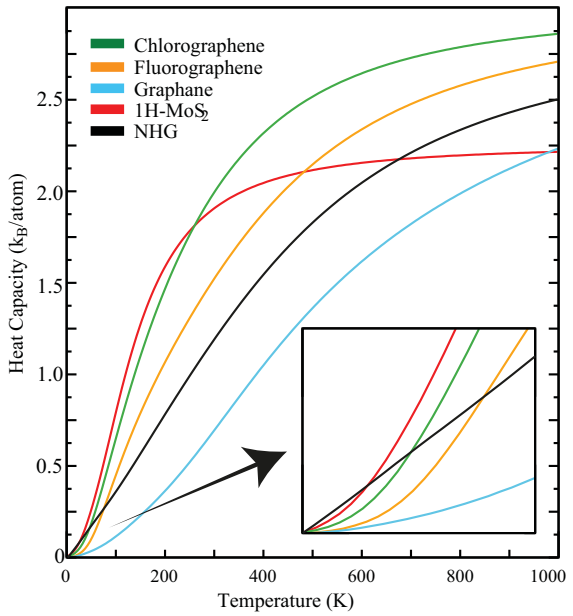


FIG. 5. (Color online) Constant-volume heat capacity of atomically thin monolayer crystal structures of NHG, fluorographene, chlorographene and graphane, and $MoS_2$.

conclude that the low-temperature behavior of the specific heat of NHG is mainly determined by the ZA mode (shown in Fig. 3), which has a quadratic dispersion. Clearly, compared to other graphene derivatives, NHG displays more graphenelike thermal properties.

### A. Effect of disorder

The two-dimensional monolayer structure of graphenelike crystal structures such as NHG provide an ideal ground for monitoring the effect of atomic-scale disorders. Regarding the experimental procedure (beginning with the reaction between hexaaminobenzene trihydrochloride and hexaketocyclohexane octahydrate) of synthesis of NHG fragments, among the various disorder types formation of N-vacant lattice sites and the presence of H substitutes are more likely to occur.

Careful structure optimizations revealed that the structural deformation that stems from N vacancy is compensated by the local reconstruction of four neighboring carbon atoms (per primitive unit cell). It is seen from Fig. 6(a) that upon the formation of a double covalent bond at a N-vacant lattice site two benzene rings are linked via a pentagonal ring. We reported formation of similar reconstructions in trigonally arranged nanomeshes of $C_2$, $C_4$, and $C_{12}$ holes in graphene [5], However, as shown in Fig. 6(b), in the presence of H impurity local distortion is small and the hexagonal crystal symmetry of NHG does not change considerably. Here it is noteworthy to mention that the density of missing N and H impurity is very high, and for lower density of impurities, lattice distortion becomes negligible.

The electronic density of states of disordered NHGs presented in Fig. 6(c) shows that the presence of N vacancies results in hole doping and the NHG crystal shows metallic behavior. However, although the presence of H impurities leads to a significant decrease in the electronic band gap, NHG

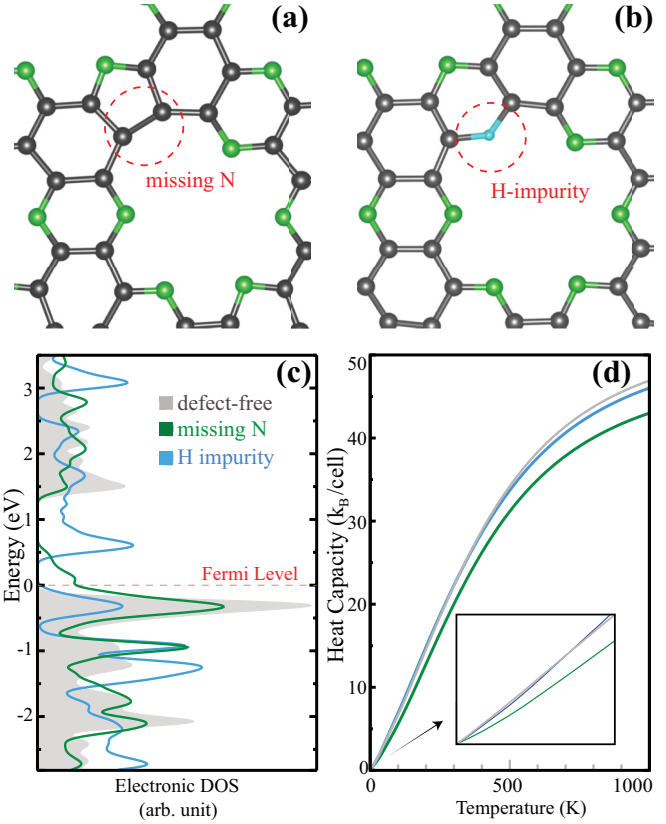


FIG. 6. (Color online) Structure of possible disorders (a) missing N atom and (b) H impurity and their effects in electronic DOS and constant-volume heat capacity.

crystal keeps its semiconducting nature. In Fig. 6(d) we also show how the constant-volume heat capacity of NHG crystal is affected by the presence of H impurity and N defects. While the $C_V$ of N-defected crystal has a quadraticlike behavior at low temperatures, H impurity, including crystal, has almost the same temperature dependency with disorder-free NHG. It appears that both disorder types have a negligible effect on the thermal property of NHG crystal, even in the high-concentration disorder case.

## VI. CONCLUSIONS

In this study structural and vibrational properties of recently synthesized NHG crystal were investigated. Our charge density analysis revealed that positively charged holey sites of NHGs can be further utilized for functionalization by adatom and molecule groups. Formation of nitrogen-functionalized holey graphene not only leads to a band-gap opening in graphene's electronic band dispersion, but also provides a crystal structure as stable as graphene. In addition, further analysis of the vibrational characteristics also revealed that the NHG crystal structure has some distinctive phonon modes in its Raman spectrum. We also found that the specific heat of the NHG has a linear dependence to temperature at low temperatures and it obeys the Dulong-Petit law at high temperatures. Moreover, we found that while the presence

of H and N disorders significantly modifies the electronic properties, their effect on phononic properties of NHG is negligible. Our calculations also revealed that for nanodevice applications, NHGs can be favored over the other graphene derivatives and 1H-$MoS_2$.

**ACKNOWLEDGMENTS**

Computational resources were provided by TUBITAK ULAKBIM, High Performance and Grid Computing Center (TR-Grid e-Infrastructure). H.S. is supported by a FWO Pegasus Long Marie Curie Fellowship.

[1] K. S. Novoselov, A. K. Geim, S. V. Morozov, D. Jiang, Y. Zhang, S. V. Dubonos, I. V. Grigorieva, and A. A. Firsov, Science **306**, 666 (2004).
[2] H. Lu and S.-D. Li, J. Mater. Chem. C **1**, 3677 (2013).
[3] J. Lahiri, Y. Lin, P. Bozkurt, I. I. Oleynik, and M. Batzill, Nat. Nanotechnol. **5**, 326 (2010).
[4] J. Bai, X. Zhong, S. Jiang, Y. Huang, and X. Duan, Nat. Nanotechnol. **5**, 190 (2010).
[5] H. Sahin and S. Ciraci, Phys. Rev. B **84**, 035452 (2011).
[6] E. L. Spitler and W. R. Dichtel, Nat. Chem. **2**, 672 (2010).
[7] J. W. Colson and W. R. Dichtel, Nat. Chem. **5**, 453 (2013).
[8] A. P. Cote, A. I. Benin, N. W. Ockwig, M. O'Keeffe, A. J. Matzger, and O. M. Yaghi, Science **310**, 1166 (2005).
[9] S. Kandambeth, D. B. Shinde, M. K. Panda, B. Lukose, T. Heine, and R. Banerjee, Angew. Chem., Int. Ed. **52**, 13052 (2013).
[10] J. Mahmood, E. K. Lee, M. Jung, D. Shin, I.-Y. Jeon, S.-M. Jung, H.-J. Choi, J.-M. Seo, S.-Y. Bae, S.-D. Sohn, N. Park, J. H. Oh, H.-J. Shin, and J.-B. Baek, Nat. Commun. **6**, 6486 (2015).
[11] P. E. Blöchl, Phys. Rev. B **50**, 17953 (1994).
[12] G. Kresse and J. Hafner, J. Phys. Rev. B **47**, 558(R) (1993).
[13] G. Kresse and J. Furthmüller, Phys. Rev. B **54**, 11169 (1996).
[14] G. Kresse and D. Joubert, Phys. Rev. B **59**, 1758 (1999).
[15] J. P. Perdew, K. Burke, and M. Ernzerhof, Phys. Rev. Lett. **77**, 3865 (1996).
[16] R. F. W. Bader, *Atoms in Molecules – A Quantum Theory* (Oxford University Press, Oxford, UK, 1990).
[17] G. Henkelman, A. Arnaldsson, and H. Johnson, Comput. Mater. Sci. **36**, 354 (2006).
[18] D. Alfe, Comput. Phys. Commun. **180**, 2622 (2009).
[19] S. Tongay, H. Sahin, C. Ko, A. Luce, W. Fan, K. Liu, J. Zhou, Y. S. Huang, C. H. Ho, J. Yan, D. F. Ogletree, S. Aloni, J. Ji, S. Li, J. Li, F. M. Peeters, and J. Wu, Nat. Commun. **5**, 3252 (2014).
[20] H. Sahin, S. Tongay, S. Horzum, W. Fan, J. Zhou, J. Li, J. Wu, and F. M. Peeters, Phys. Rev. B **87**, 165409 (2013).
[21] H. Sahin, S. Cahangirov, M. Topsakal, E. Bekaroglu, E. Akturk, R. T. Senger, and S. Ciraci, Phys. Rev. B **80**, 155453 (2009).
[22] H. Sahin and S. Ciraci, J. Phys. Chem. C **116**, 24075 (2012).
[23] H. Sahin and F. M. Peeters, Phys. Rev. B **87**, 085423 (2013).
[24] A. A. Balandin, Nature Mater. **10**, 569 (2011).